Phase diagram of vertically vibrated dense suspensions

Stefan von Kann, Jacco H. Snoeijer, and Devaraj van der Meer

Articles you may be interested in

Microdynamics of dense colloidal suspensions and gels under constant-stress deformation
J. Rheol. **58**, 1419 (2014); 10.1122/1.4880676

Revisit to phase diagram of poly(N-isopropylacrylamide) microgel suspensions by mechanical spectroscopy
J. Chem. Phys. **140**, 024908 (2014); 10.1063/1.4861426

The role of dilation and confining stresses in shear thickening of dense suspensions
J. Rheol. **56**, 875 (2012); 10.1122/1.4709423

Shear thickening in densely packed suspensions of spheres and rods confined to few layers
J. Rheol. **54**, 1023 (2010); 10.1122/1.3474580

Static structure factor of a suspension of charge-stabilized colloids: Application to liquid-glass transition phase diagram and to micellar solution
J. Chem. Phys. **110**, 7433 (1999); 10.1063/1.478645

2014 Special Topics

PEROVSKITES
2D MATERIALS
MESOPOROUS MATERIALS
BIOMATERIALS/ BIOELECTRONICS
METAL-ORGANIC FRAMEWORK MATERIALS

AIP | APL Materials

Submit Today!

Phase diagram of vertically vibrated dense suspensions

Stefan von Kann, Jacco H. Snoeijer, and Devaraj van der Meer
Physics of Fluids Group, University of Twente, P.O. Box 217, 7500 AE Enschede,
The Netherlands

When a hole is created in a layer of a dense, vertically vibrated suspension, phenomena are known to occur that defy the natural tendency of gravity to close the hole. Here, an overview is presented of the different patterns that we observed in a variety of dense particulate suspensions. Subsequently, we relate the occurrence of these patterns to the system parameters, namely, the layer thickness, the particle concentration, and the shaking parameters. Special attention is given to the geometric properties of the particles in the various suspensions such as shape and particle size distribution. We observe these properties to be crucial for selecting the dynamics of the vibrated suspension. © *2014 AIP Publishing LLC*. [http://dx.doi.org/10.1063/1.4900855]

I. INTRODUCTION

Concentrated particulate suspensions consist of a homogeneous fluid containing particles larger than one micrometer, so that Brownian motion is negligible. They can be found in many places, and their flow is important in nature, industry, and even health care.[1] In spite of their significance, many aspects of the flow of dense suspensions remain poorly understood. In order to study these materials, people have used methods inspired by classical rheology, and typically characterized the systems in terms of a constitutive relation of stress versus shear rate.[2–6] A general result is that, when increasing the shear rate, dense suspensions first tend to become less viscous (shear thinning) and subsequently shear thicken.

Probably the most conspicuous example of a dense suspension is formed by a high concentration of cornstarch in water. One could actually run over a bath filled with a cornstarch suspension, but one would sink when standing still.[7] This is caused by solidification, activated by impact.[8] Rheological experiments in cornstarch have revealed the existence of a large shear-thinning regime that terminates in an extremely sudden shear thickening,[9] which has subsequently been interpreted as a (transient) solidification or jamming of the particle phase in the suspension. In other rheological experiments, people found a mesoscopic length scale,[5, 10] a dynamic jamming point,[4] and fracturing.[11]

Not only is the rheology of cornstarch suspensions very distinct, but unexpected phenomena were also found in experiments beyond the classical rheological ones. In experiments in which an object was left to sink into a cornstarch suspension, non-monotonic settling was observed,[12] together with the formation of a jammed region between the object and container bottom.[12, 13] Merkt *et al.*[14] observed in a vertically shaken, thin layer of cornstarch suspension that, amongst other exotic phenomena, stable oscillating holes can be formed at certain frequencies and amplitudes.[14] These were subsequently described using a phenomenological model based on a hysteretic constitutive equation.[15] Similar stable holes have not been reported in other suspensions, except for Ref. 14, where they were also found in glass bead suspensions. In potato starch and glass bead suspensions, Ebata *et al.* found self-replicating holes, and a separated state, respectively.[16, 17] They attributed the separated state to a convection-like flow, the origin of the self-replicating holes has remained unexplained. Stable holes and kinks (which are markedly similar to the separated state of Refs. 16, 17) have recently also been observed in emulsions.[18] Since emulsions do not shear thicken, this indicates that hole formation is unrelated to shear thickening. It is fair to conclude that at present we are still far from a quantitative understanding of why the above phenomena occur, and why different suspensions may behave differently.

26, 113302-1

The purpose of this work is to make an extensive inventory of the different phenomena that can occur in various vertically shaken dense particulate suspensions and in what sense cornstarch suspensions occupy a unique position amongst them. We will do this by subjecting several suspensions, including several of the suspensions mentioned before, to vertical vibrations. We then observe, describe and, whenever possible, explain the different phenomena. For cornstarch, we present a wider range of variables, including layer depth and packing fraction, which actually leads to the observation of some hitherto unreported phenomena. From the experiments with other particles, we find a dependence of particle properties on the observed phenomena.

This paper is organized as follows: In Sec. II, the experimental setup and working procedure are introduced, after which we present the various phenomena we observe in a variety of vibrated suspensions in Sec. III. After that, in Sec. IV, we will quantify how these phenomena depend on the concentration, layer depth, and shaking parameters. Here, we will use cornstarch as our "benchmark" material and relate the properties of the other particles used in suspension to those of cornstarch. Section V will conclude the paper.

II. EXPERIMENTAL SETUP AND PROCEDURE

A. Setup

The experimental setup is shown in Fig. 1. Its core consists of a cylindrical container with a diameter $D = 11.0$ cm and a height H of 8.0 cm. This container is vertically vibrated by a shaker (TiraVib 50301) with frequencies f between 20 and 200 Hz and a dimensionless acceleration Γ from 0 up to 60. Here, $\Gamma = a(2\pi f)^2/g$, where a is the shaking amplitude and g the gravitational acceleration. Like any electromagnetic shaker, the parameter range attainable by the TiraVib 50301 is limited in amplitude (<12.8 mm), velocity (<1.5 m/s), and acceleration ($<110g$). The container is filled up to a variable height h between 4 and 20 mm with a suspension of varying composition. The suspension layer in the container is recorded with a high speed camera at various frame rates, given in frames per second (fps), and is either imaged from the side or from the top.

B. Procedure

Suspensions consist of a suspending liquid and particles. However, mixing two arbitrary constituents of these types does not always lead to a stable suspension. When particles are hydrophilic, a suspension can be made using water, but for hydrophobic particles we have to turn to other suspending liquids. Even when a suitable suspending liquid has been found, particles denser than the liquid are likely to sediment, such that a density matching agent needs to be used. We used a variety of particles to create our suspensions, each with their own properties, an overview of which is presented in Table I. A more detailed description of each suspension can be found in the experimental part, where their properties will be discussed in relation to the experimental results.
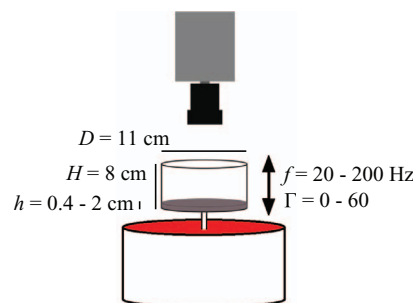
FIG. 1. A schematic view of the used setup. At the lower end we have the shaker, on top of which the container with the suspension is mounted, which is subsequently vibrated vertically. The dynamics of the suspension is captured from above using a high speed camera.

TABLE I. Schematic overview of the particles and their properties, used in this study. The polystyrene beads have a sharply peaked, quite monodisperse distribution. Cornstarch has a flat size distribution which stands for roughly equal numbers of particles for every size. The glitter particles are rectangular and have a size of 50×50, 50×75, and 50×100 μm and a thickness of 20 μm. Data are given for the 50×50 μm particles. The glass beads and quartz flour particles have a very broad size distribution, consisting mainly of smaller particles and a strongly decreasing number of particles when going to larger sizes. We will refer to these very broad size distributions as polydisperse.

Particles	Size (μm)	Range (μm)	Density (kg/m^3)	Shape	Suspending liquid
Cornstarch	17 (30%)	5–25	1.7×10^3	Edgy	Demi water
Glitter	50 (10%)	45–55	1.5×10^3	Flat rectangles	Sunflower oil
Polystyrene beads	22 (5%)	20–38	1.05×10^3	Spherical	Demi water
Glass beads	4 (200%)	0–20	2.5×10^3	Spherical	Demi water
Quartz flour	30 (150%)	0–75	2.5×10^3	Edgy	Demi water

For the hydrophilic particles, we used demineralized water as the suspending liquid, but the particles are typically more dense than water. When this density contrast is large (e.g., glass in water) density matching of the liquid is required. To this end, we used two different salts: Cesium Chloride (CsCl) for densities up to 1.8×10^3 kg/m^3 and Sodium Polytungstate (Na$_6$[H$_2$W$_{12}$O$_{40}$]) for densities up to 2.5×10^3 kg/m^3. We observed however that slight variations in density matching did not significantly change the observations reported in this study. Some of our particles are hydrophobic, making water unsuitable as the suspending liquid. For suspending these particles we used sunflower oil. An important parameter for our suspensions is the concentration, which we express as the volume fraction ϕ that is occupied by the solid phase in the suspension. In this work, we will concentrate on dense suspensions, and it should be kept in mind that all of the described phenomena will disappear when the suspension is sufficiently diluted.

For the suspensions (and the quite viscous Newtonian liquids) we have used in our container, and for the shaking amplitudes and frequencies used in this study, the vibrated fluid is usually quite undisturbed. The liquid surface is typically smooth, on top of which, if the shaking conditions are favorable, we may observe Faraday waves[19] of very small wavelength. The phenomena we report in this work occur only after a manual disturbance has been made in the liquid. This was either done by puffing air into the layer using a straw, or by poking a hole into the fluid with a stick. Here we note that, apart from the fact that small disturbances tend to flatten out, the size of the initial disturbance is of little consequence for the observed phenomena. For example, a bigger initial destabilization will not shift the boundary between stable and unstable holes in the phase diagram.

III. PHENOMENOLOGY

In this section, we will describe the several possible states and phenomena we observe after the initial perturbation has been created in the liquid.

A. Newtonian liquid

Let us first briefly discuss what happens when a very viscous Newtonian liquid is vibrating vertically, and a perturbation is created in the form of a hole. To this end, we put a layer of honey with a thickness $h = 6$ mm and a dynamic viscosity $\mu \approx 6.3$ Pa s in our setup. Without vibration, the hole will collapse under the influence of hydrostatic pressure. The same happens when the layer is vibrated and a hole is created, only now we observe that the edges of the hole oscillate along with the driving frequency. In Fig. 2, we plot the time evolution of the diameter of the hole and observe that the diameter actually decreases approximately linearly in time. On top of this decrease, we observe an oscillation at the same frequency as that of the shaker.
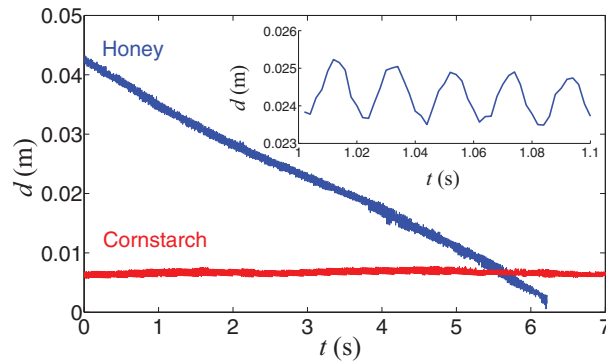
FIG. 2. Comparison of the time evolution of the diameter of a hole created in a layer of honey of thickness $h = 6$ mm which is vibrated at a frequency $f = 50$ Hz and a dimensionless acceleration $\Gamma = 30$, recorded at 250 fps, and that of a stable hole created in a layer of cornstarch suspension ($h = 7$ mm; $\phi = 0.40$) at $f = 100$ Hz and $\Gamma = 20$, recorded at 500 fps. The inset shows a few cycles from the experiment in honey (at 500 fps), clearly showing the oscillations of the edge with the driving frequency.

B. Cornstarch suspensions

Contrary to Newtonian fluids, in suspensions hydrostatic pressure can be overcome dynamically due to the imposed vibration. The hole will not (fully) close, and a rich variety of phenomena can be observed. The richest phenomenology is found in cornstarch suspensions, where upon varying our experimental parameters we found four different phenomena. In accordance with the existing literature, we denote these two phenomena as stable holes, and fingers.[14] We also found two unreported phenomena which we will call rivers, and jumping liquid. From each of these states, a snapshot can be found in Fig. 3. We will now discuss the characteristics of these phenomena in detail.

1. Stable holes

When an initial perturbation develops to a circular hole of constant average diameter, we speak of a stable hole [see Fig. 3(a)]. In the vertical direction such a hole typically extends to the bottom of the container, and the hole edge oscillates along with the driving frequency.

Merkt *et al.*[14] attributed the stability of the holes in the cornstarch suspension to shear thickening. They found that typical shear rates in the shaking experiments were around the same value for which a sudden shear thickening was observed in rheometer experiments. Deegan[15] proposed a one-dimensional hysteretic model to explain why these holes do not collapse due to hydrostatic pressure. In this model, he proposed a coexistence of two stable branches in the stress versus strain
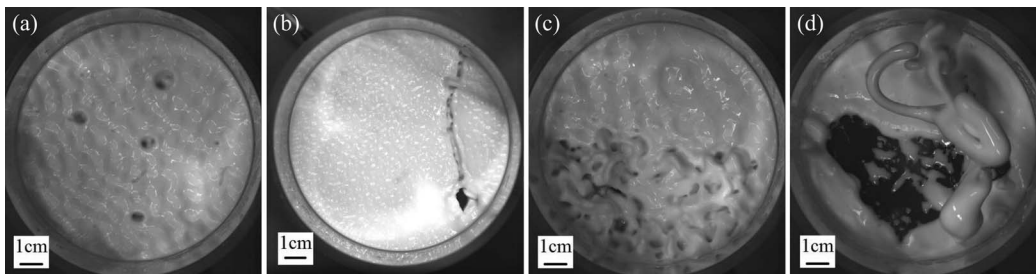
FIG. 3. Snapshots of the four different phenomena that can be observed in a vertically vibrated layer of cornstarch suspension. From left to right: (a) Holes in a suspension layer of thickness $h = 6$ mm and with a concentration $\phi = 0.4$, shaken at $f = 80$ Hz and $\Gamma = 20$. (b) River in a $\phi = 0.38$ suspension with $h = 6$ mm, shaken at $f = 140$ Hz, $\Gamma = 40$. (c) Fingers in a $\phi = 0.4$ suspension with $h = 6$ mm, shaken at $f = 80$ Hz with $\Gamma = 30$. (d) Jumping liquid, just after its release from the vibrated layer, in a $\phi = 0.4$ suspension with $h = 6$ mm, shaken at $f = 40$ Hz, $\Gamma = 40$.

rate diagram. Based on this, it was argued that the edge of the hole will move inward only slightly during the first half of the cycle (large shear stress), but will then jump to the lower branch such that during the outward motion the suspension experiences a smaller shear stress, resulting in a larger outward displacement. In the one-dimensional model, this actually lead to growing holes, but one could imagine that a stable equilibrium radius would be found for the two-dimensional, radially symmetric problem that corresponds to the experiment.

In more recent experiments by Falcón *et al.*,[18] the stability of holes in a vibrated emulsions was connected to the normal stress caused by a convection roll in the rim that surrounds the hole. We verified that such a roll is also visible in the rim around the holes in our cornstarch suspensions by putting tracer particles in the hole, which came out along the rim of the hole.

2. Rivers

In cornstarch suspensions with lower concentrations ϕ, we observe the formation of an elongated structure [Fig. 3(b)], which has not been reported before. Due to its shape we denote these from here on as rivers. Also the rivers start from a single perturbation in the suspension, but now the original hole tends to slowly stretch out or "walk" through the suspension. When the river reaches the container wall, it leaves an entire line-shaped structure (or even multiple lines) behind that penetrates the suspension layer all the way to the bottom of the container. The directionality appears to be random. As soon as this river touches the container edges it stabilizes and, just like the stable holes it has a very long lifetime: the structure easily outlives the duration of the experiment, which was typically in the order of $10^5 - 10^6$ cycles.

3. Fingers

Fingers [see Fig. 3(c)] are formed at higher shaking strengths. In this regime, the small rim on the edge of the hole increases in size and "lifts off" from the surface. Eventually, the fingers fall down and form new holes, which again grow new fingers. These fingerlike protrusions were also reported by Merkt *et al.*[14]

4. Jumping liquid

The fingers described in the previous paragraph become larger when, at constant Γ, the amplitude is increased. For sufficiently large amplitude, the connection to the surface may break while the finger is growing, and a "blob" of suspension will start jumping around in the container [see Fig. 3(d)]. Eventually, it will form into a spherical shape, and with every bounce on the suspension surface, it slowly shrinks in size over a timespan of minutes. Below a certain size this sphere will coalesce with the surface, a process which either causes a new hole-shaped disturbance to form – eventually leading to the growth of a new amount of jumping liquid – or the sphere is simply absorbed after which the process stops. In order to investigate the packing fraction of the detached balls, we have caught several of these blobs of suspension in flight. It was found that the concentration varied by a few percent, but with an average that was equal to the bulk packing fraction.

C. Other suspensions

Starting from the hypothesis that it is the geometrical shape of the cornstarch particles in the suspension that is responsible for the large variety of phenomena that can be observed in vertically vibrated cornstarch suspensions, we examined a variety of other dense particulate suspensions, with varying geometrical parameters. We did not however, succeed in creating a suspension that presented similar phenomena as cornstarch. The other suspensions we studied have an interesting phenomenology as well, but it is markedly different from that of cornstarch: Steady states like the stable holes and rivers are absent; instead, we find much more dynamic phenomena like the growing and splitting holes we will describe below.
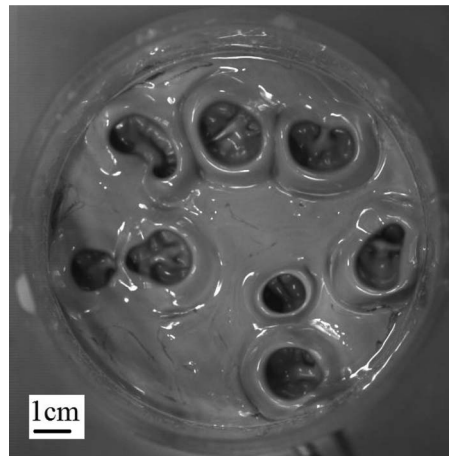
FIG. 4. Splitting holes in a vibrated polydisperse glass bead suspension with an average diameter of 10 μm ($f = 100$ Hz, $\Gamma = 25$, $h = 7$ mm, and $\phi = 0.60$).

1. Splitting holes

After creating an initial disturbance in a suspension containing polydisperse particles, we observe a hole that immediately starts to grow and quickly departs from the circular shape: The hole tends to stretch out and eventually splits up into two circular holes. These in turn again grow and become non-circular, leading to another splitting up. This way new holes are formed very rapidly, and as soon as the system is full of holes they are also observed to collide and merge or to fully close. The timescale of the dynamics of splitting and colliding depends strongly on particle type and shaking parameters, and can range from a few seconds up to several minutes. This eventually leads to a very chaotic dynamics. A snapshot of a container with several of these holes can be found in Fig. 4.

2. Growing holes and kinks

In particle suspensions with a narrow to moderate size distribution, the phenomenology turned out to be very different again. After creating the initial disturbance, a circular hole is formed. Depending on the shaking strength and amplitude we find two phenomena. At the lower end, we observe a hole that grows until a maximum size is reached. After this it rapidly collapses to a very small size and a growth phase sets in again. When shaking harder, the hole will grow until it hits the container wall. In this case, the hole will open up and form a large dry area at the container bottom, thus creating a system that is partly covered with a thick layer of suspension, partly dry, and an abrupt transition between them which is called a kink.[18] Snapshots of such a series of events can be found in Fig. 5. The distinction between the two states is not always very clear, since in some cases the hole size will saturate, the entire hole will keep on moving slowly inside the container, and eventually come in contact with an edge, which then leads to the formation of a kink. The time span for this to happen however, can be minutes whereas the kink formation described above typically happens within seconds.

IV. QUANTITATIVE RESULTS

Which of the above mentioned phenomena we observe depends on the composition of the suspension, its packing fraction ϕ, the depth of the layer h, as well as the shaking parameters frequency f and shaking strength Γ. In this section, we present the results of the experiments done with the various suspensions, and discuss them for each suspension by means of phase diagrams of the shaking parameters Γ and f.
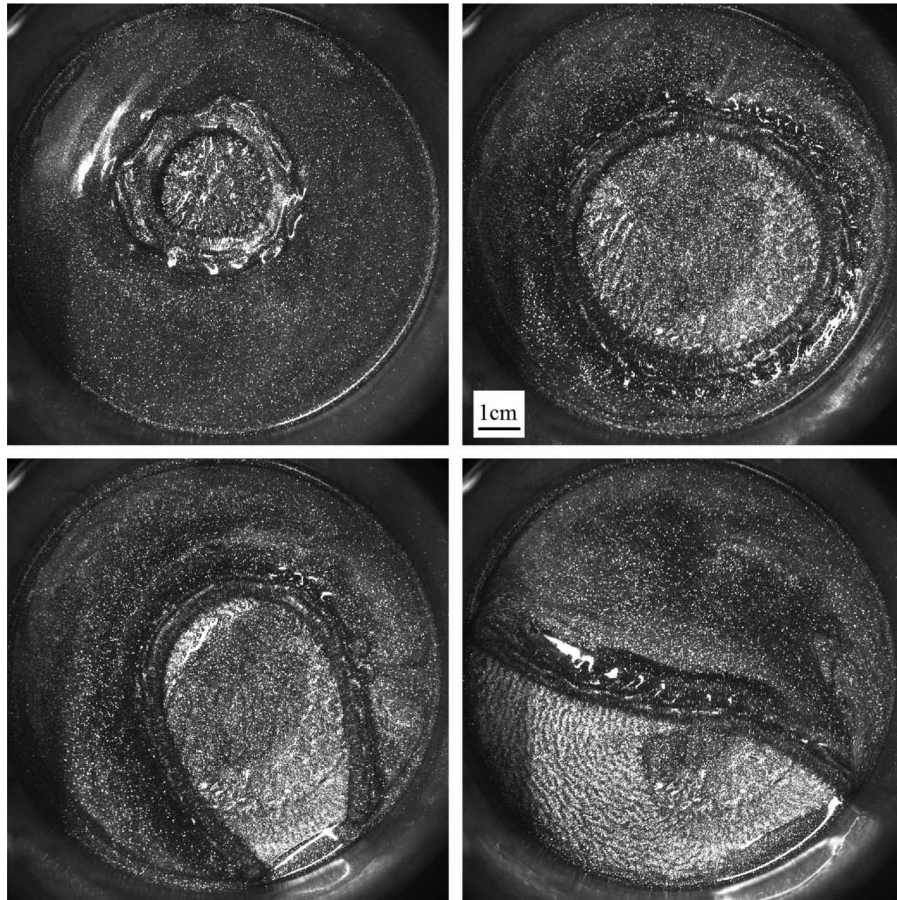
FIG. 5. Four snapshots of the development of a hole towards a kink in a suspension of glitter particles. The frames go from top left to bottom right and are at $t = 1, 60, 73$, and 92 s after the creation of the initial hole ($f = 80$ Hz, $\Gamma = 30$, $h = 7$ mm, and $\phi = 0.60$).

A. Cornstarch

As cornstarch has proven to have the richest phenomenology, we will start with the discussion of our experiments in cornstarch suspensions. Previously, these type of shaken suspensions have been considered by Merkt *et al.*[14] Their report, however, was limited to a single set of experiments with a fixed depth and packing fraction, in which only the shaking parameters were varied. Our objective here is to map out a larger part of the parameter space by in addition varying the layer depth and concentration. More specifically, we want to determine how the phenomena described in Ref. 14 (holes and fingers) are influenced by these other parameters, and how the newly described rivers and jumping liquid fit into the phase diagrams.

We use either demineralized water or an aqueous solution of Cesium Chloride (CsCl) with a density of $\approx 1.7 \times 10^3$ kg/m^3, matching the cornstarch particle density (based on sedimentation experiments: At $\rho = 1.7 \times 10^3$ kg/m^3 cornstarch particles do not settle to the bottom for several days). Experiments actually showed negligible differences between results in the density-matched and the unmatched liquid, presumably due to the relatively violent shaking. In the unmatched suspension only some stirring is required just before the start of a new experiment, to counteract sedimentation. Viewing the cornstarch particles under a microscope, see Fig. 6, reveals that they are irregularly shaped and have an approximately flat size distribution in the range of 5–20 μm.

The first parameter we studied is the packing fraction ϕ at a fixed layer depth of $h = 6$ mm. For packing fractions up to and including $\phi \approx 0.35$, we find that any perturbation closes due to hydrostatic pressure, as would happen in a Newtonian liquid. At the slightly higher value
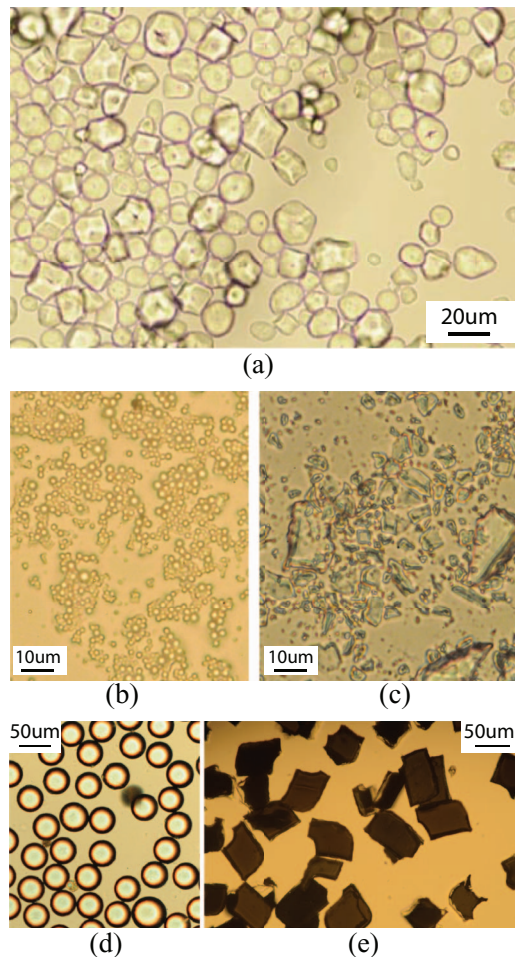
FIG. 6. Microscopic pictures of the various particles that were used in this study: (a) cornstarch (particle diameter $\sigma = 5–25$ μm); (b) polydisperse glass beads ($\sigma = 0–20$ μm); (c) quartz flour $\sigma = 0–75$ μm; (d) monodisperse polystyrene beads ($\sigma \approx 40$ μm); (e) a mixture of glitter particles (dimensions 50×50 μm^2, 50×75 μm^2, and 50×100 μm^2, respectively, each with a thickness of 20 μm). See Table I and the Appendix for further details.

$\phi = 0.38$, we observe closing holes for low shaking strengths (up to $\Gamma = 25$), indicated by the plus symbols and the white background in the phase diagram of Fig. 7(a). At relatively high accelerations ($\Gamma = 40$) and low frequencies (80 Hz), we observe fingerlike shapes emerging from the rim of the disturbance, indicated by the dots and the light grey background. These fingerlike shapes were also reported by Merkt *et al.*[14] for high shaking strengths. At higher frequencies, we observe that the created holes are not stable but tend to stretch out and form riverlike structures [the diamonds and dark grey background in Fig. 7(a)]. These rivers spread out over the entire width of the container and then become stable. When increasing Γ at constant *f*, the edge of the rivers rise up and again form fingerlike structures.

In the phase diagram at intermediate volume fraction, $\phi = 0.40$, we find that the onset of the fingers and rivers regimes shifts to lower shaking strengths [Fig. 7(b)]. Below this onset, there now exists an additional narrow window in which stable holes form (represented by circles and medium grey background). That is, increasing the acceleration Γ for frequencies around 80 Hz we first observe the formation of stable holes which then give way to fingerlike structures at higher Γ. When we increase Γ at higher frequencies (around 130 Hz), stable holes first turn into rivers which subsequently will produce fingers that will eventually cover the entire surface for the highest values of Γ.
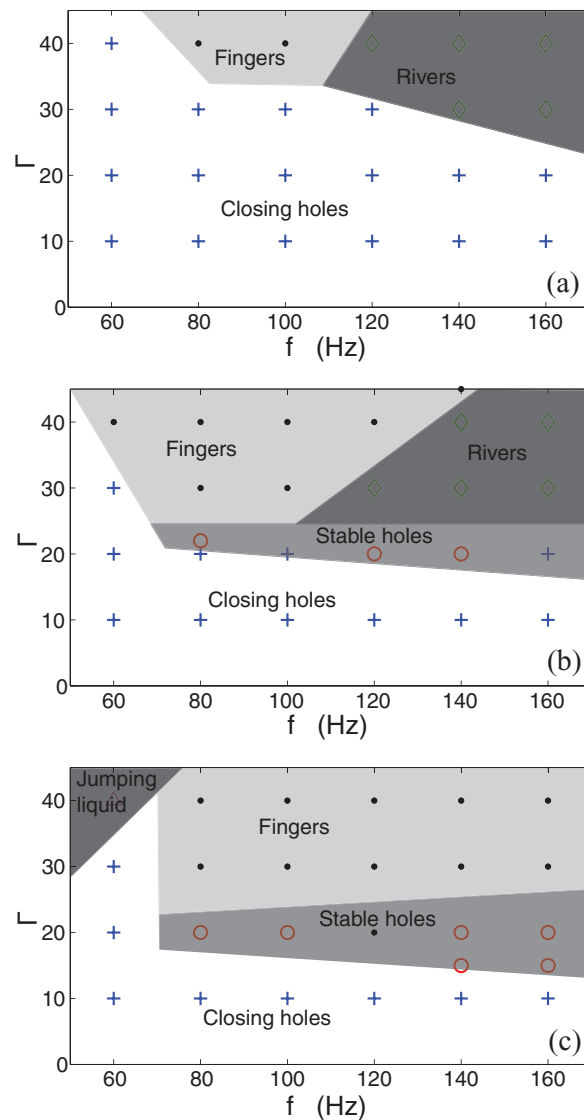
FIG. 7. Phase diagrams in the plane spanned by the shaking parameters frequency f and dimensionless acceleration Γ for three different cornstarch suspension concentrations ϕ. From top to bottom: (a) $\phi = 0.38$; (b) $\phi = 0.40$; and (c) $\phi = 0.42$. In all three diagrams, we used a fixed layer depth of $h = 6$ mm. The colored areas are added as a guide to the eye and roughly indicate the various regimes in which the phenomena are visible.

When increasing the packing fraction even further, to $\phi = 0.42$, the onset of the stable holes regime continues to shift to lower shaking strengths [Fig. 7(c)]. In addition, rivers are no longer encountered in the phase diagram: The stable holes always give rise to finger formation when Γ is increased. Besides the holes and fingers, there is one additional phenomenon: In the finger regime, when we decrease the frequency at a fixed, high shaking acceleration – i.e., when the amplitude of the shaker is increased – the fingers tend to rise up higher and at a certain point they actually break loose of the surface and form jumping shapes that can live for several thousands of cycles of the driving. This jumping liquid regime is represented by triangles and a dark grey background in the phase diagram.

The second parameter whose influence we will study in detail is the layer depth h. To this end, we choose a fixed high packing fraction of $\phi = 0.41$, for which the phase diagrams are particularly rich. Since Merkt et al.[14] used a fixed layer depth of 5 mm, we start at the slightly lower value of
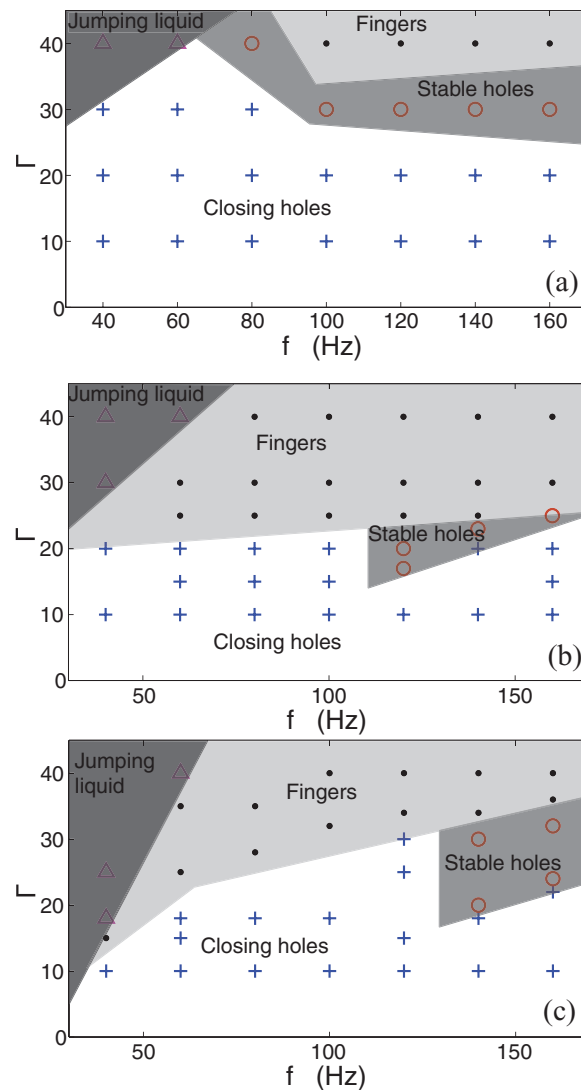
FIG. 8. Phase diagrams for three different cornstarch layer thicknesses. From top to bottom: (a) $h = 4$ mm, (b) $h = 10$ mm, and (c) $h = 14$ mm, all at a concentration of $\phi = 0.41$. The colored areas are added as a guide to the eye and roughly indicate the various regimes in which the phenomena are visible.

$h = 4$ mm, and increase the depth to $h = 10$ and $h = 14$ mm (with the intermediate value of $h = 6$ mm covered in Figs. 7(b) and 7(c) for slightly different values of the concentration ϕ). The resulting phase diagrams are presented in Fig. 8.

In this figure, we see that the types of observed phenomena do not vary with the layer depth, but that the regions in parameters space in which they occur do vary in size and position. First, we find that the onset of the phenomena moves down in acceleration Γ with increasing layer depth. Second, we observe that the region in which stable holes are encountered both decreases in size and moves to higher shaking frequencies. In even deeper layers than the ones presented in Fig. 8 no stable holes are formed at all. This is most likely due to the fact that hydrostatic pressure becomes more important as the layer depth increases. A stable equilibrium between the effect of the shaking and hydrostatic pressure is then either not possible or happens at such high frequency/acceleration combinations that the regime is not attainable with our experimental setup. The regimes in which fingers and jumping liquid are found increase with layer depth, mainly due to a shift of the onset
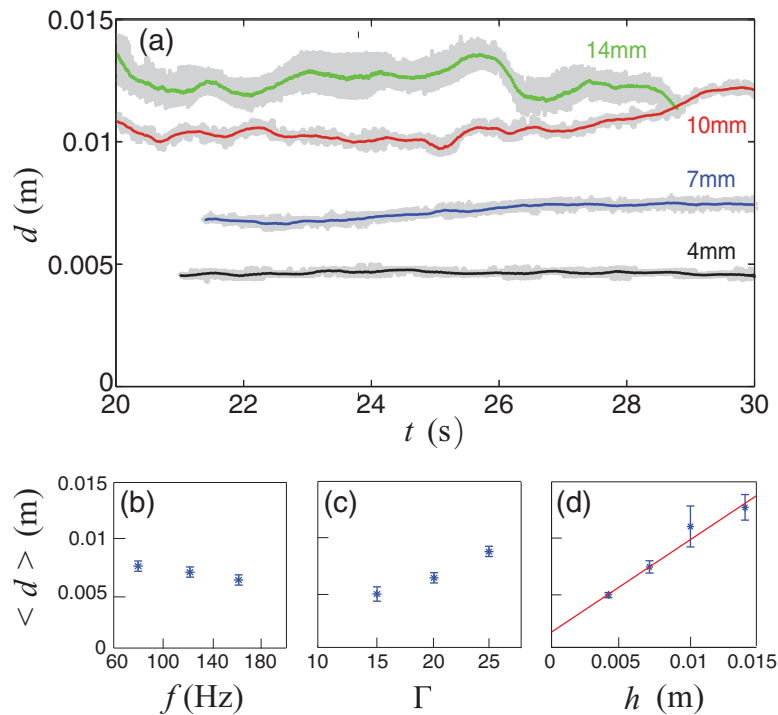
FIG. 9. (a) Time evolution of the hole diameter d for four different values of the layer depth ($h = 4, 7, 10, 14$ mm) and $\phi = 0.41$. The (grey) traces indicate the periodic motion of the holes whereas the colored lines indicate the corresponding period-averaged value. (b) Time-averaged diameter $\langle d \rangle$ as a function of the frequency f (for $\Gamma = 20$, $h = 6$ mm, and $\phi = 0.40$). (c) $\langle d \rangle$ as a function of Γ ($h = 6$ mm, $f = 160$ Hz, and $\phi = 0.40$). (d) $\langle d \rangle$ as a function of layer depth h for $\phi = 0.41$, together with a linear best fit. The data of this last plot necessarily had to be obtained using different values for Γ and f, as explained in the main text.

towards smaller Γ for larger h. For very large layer depth, sometimes it appears that fingers can form while the empty space between the fingers does not reach the bottom.

Finally, we will discuss how the size of the holes in the stable hole regime depends on the various parameters of the system. Note that this task is complicated by the fact that the shape and contours of the stable hole regime depend on these parameters in a rather non-trivial manner (cf. Figs. 7 and 8). To this end, we use the time series of the hole diameter obtained with our high-speed camera (Fig. 9(a)) to determine the time-averaged diameter $\langle d \rangle$ of the hole.

Turning first to the dependence of $\langle d \rangle$ on the frequency of the driving [Fig. 9(b)], we observe a very slight decrease in hole size with increasing f, while keeping Γ and h fixed. This dependence however is only small compared to other dependencies: The average hole diameter significantly depends on the shaking acceleration [see Fig. 9(c)], where a larger acceleration leads to larger holes, when all other parameters are held constant. The increase is such that with an increase of $10g$ the hole almost doubles in diameter. In addition, the hole size also strongly depends on the layer depth. In Fig. 9(d), we see that the layer depth h clearly sets the average hole diameter $\langle d \rangle$ as both quantities appear to be proportional to one another. This proportionality is however hard to establish experimentally as a single value for the parameter pair f and Γ for which stable holes develop for different layer depths could not be found. We therefore had to use slightly varying parameters ($f = 140$ Hz and $\Gamma = 30$ for the $h = 4$ mm experiment, $f = 120$ Hz and $\Gamma = 20$ for both the $h = 7$ and the $h = 10$ mm experiments, and $f = 160$ Hz and $\Gamma = 24$ for the $h = 14$ mm experiment). This slight variation in shaking parameters might explain why the points do not fall onto a single line through the origin. Turning back to the time evolution of the hole diameter [Fig. 9(d)] we observe that for thin layers the hole appears to be more stable than for thick layers, where occasionally even multiple-valued data seem to be present. Although the increased instability (e.g., the waviness at

$h = 14$ mm appears to be physical, the multivaluedness is connected to the increased difficulty of the image analysis for larger h).

Finally, the concentration does not appear to influence the hole size. It should, however, be stated that the range in which we can vary the packing fraction ϕ and observe stable holes is not very large compared to the variation we can apply in the other parameters (cf. Fig. 7).

Cornstarch consist of edgy particles, i.e., they more resemble polygons than spheres, that have an aspect ratio close to one and a flat size distribution with diameters between 5 and 20 μm, with which we mean that particles of different sizes come in roughly equal numbers. Unfortunately, apart from cornstarch and other similar starches, it is hard to find particles made of a different material and roughly the same geometrical properties. In the remainder of this section, we therefore study the behavior of several other particle suspensions, the particles of which all differ in certain aspects from cornstarch, and compare it to the behavior of cornstarch suspensions.

B. Polydisperse glass beads

The first alternative suspension we turn to are polydisperse glass beads in various size distributions. The beads are spherical and have a density of 2.5×10^3 kg/m^3. Due to the large density contrast with water, density matching with sodiumpolytungstate is required. Initially, we used beads in the same size range as cornstarch, 0–20 μm, of which a microscopic picture can be found in Fig. 6(b). From this picture, it becomes immediately clear that there are much more small particles than large ones, and therefore the distribution is not flat like that of cornstarch, but the smaller sizes heavily dominate in numbers.

When performing the shaking experiment we observe that after creating an initial disturbance, the hole immediately starts splitting up and colliding with other holes. This splitting and colliding cycle repeats itself every few seconds, leading to a very chaotic dynamics of which a snapshot was shown in Sec. III C (Fig. 4). Next to the closing holes, this is found to be the only observable phenomenon in this type of suspension. The speed with which the holes split and collide depends on the shaking acceleration and the onset varies with the shaking frequency. A phase diagram of the behavior of the polydisperse glass beads suspension as a function of shaking acceleration Γ and frequency f is provided in Fig. 10.

Polydisperse glass beads of other size distributions, namely, 0–50 μm and 40–70 μm qualitatively have the same behavior. Varying the layer depth and the packing fraction also do not lead to different behavior or different phenomena.

As an alternative to the overwhelmingly large number of small particles present in the above samples, we used a sample with a more moderate polydispersity consisting of spherical glass beads with sizes between 20–30 μm and a more flat size distribution. Again, only splitting and closing holes are observed. The big difference with the previous samples is that it now takes up to a minute
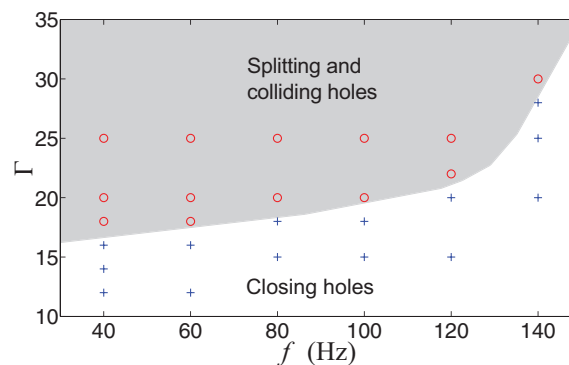
FIG. 10. Phase diagram in the (f,Γ)-plane for polydisperse glass beads with a non-flat size distribution from 0 to 20 μm. The concentration was $\phi = 0.6$ and the layer depth was fixed to $h = 7$ mm. The grey area is added as a guide to the eye and indicates the region where holes grow and duplicate, moving to a disordered state.

for a hole to start splitting. This is a lot longer than for the more polydisperse particles for which this only takes seconds.

C. Quartz flour

The second alternative to cornstarch is quartz flour, which consist of crushed quartz crystals and of which a microscopic picture can be found in Fig. 6(c). The size distribution, which ranges from 0 to 70 μm, is similar to that of the polydisperse beads mentioned above, i.e., non-flat with a very large number fraction of small particles. However, the edgy particle shape is more comparable to that of the cornstarch particles. Its density is $\approx$2.5 $\times$ 10^3 kg/m^3 and the liquid used to create a suspension is again water, density matched with sodiumpolytungstate.

The phase diagram of a vertically vibrated quartz flour suspension (not shown) is very similar to that of polydisperse glass beads: We find two possible states, namely, closing holes for low shaking accelerations and splitting holes at high values of Γ.

For both polydisperse particles, quartz flour and glass beads, filtering was attempted to reduce the surplus of small particles. We attempted several rounds of filtering, either by sieving or selective sedimentation, but it was not possible to remove the small particles to a satisfying extent, and the experimental results did not qualitatively change.

D. Monodisperse beads

In Subsections IV B and IV C, it became clear that the chaotic behavior of the polydisperse glass beads in the splitting hole state could be tempered by reducing the polydispersity of the material. It would therefore be interesting to study monodisperse glass beads, which unfortunately are costly and hard to obtain in the necessary quantities. We therefore used polystyrene beads of 20, 40, or 80 $\pm$ 5 μm (MicroBeads, TS 20-40-80), of which a microscopic picture can be found in Fig. 6(d). The particles have a density of 1050 kg/m^3 and are mixed with water to create a suspension. Due to the small density difference density matching was not necessary.

Again, for low values of Γ we find closing holes for all examined values of f. Beyond a frequency-dependent onset acceleration, we observe that the initial perturbation turns into a circular hole which grows in time without losing its circular shape. Subsequently, depending on the suspension details and the shaking parameters, the hole will either collapse due to the formation of a rising rim which grows in size while the hole is growing, or will continue to grow until it reaches the container wall and form a kink. The intricate dynamics of the hole growth will be treated in a separate paper.

E. Glitter

To combine monodispersity with a certain edginess of the particles, we finally employ glitter particles (Sigmund-Lindner, SiliGlit, Polyester Glitter, GradeII). These particles predominantly consist of polyethylene, which are edgy, and have a density of 1.38 $\times$ 10^3 kg/m^3. These particles – which incidentally are obtained by cutting of sheet material and mainly intended for use in the cosmetic industry – are available in squares, rectangles, and octagons and are relatively thin (20 μm) compared to the other dimensions (50–100 μm) In addition, they have a quite narrow size distribution. The particles are hydrophobic, so an apolar liquid needs to be used to create a suspension for which we took sunflower oil. A microscopic picture of a mixture of some of the glitter particles can be found in Fig. 6(e).

We have produced various different suspensions, either with a single size of particles, or a mixture of particles and in different concentrations, and the results were found to be qualitatively the same: A disturbance grows and eventually form a large kink covering part of the container surface. Snapshots of such a series of events had been provided in Fig. 5 and a typical phase diagram with the crossover between closing and growing holes can be found in Fig. 11. A phase diagram for the monodisperse beads discussed above would qualitatively show the same results.

The edge of the kink clearly shows a convection roll, which can be observed without adding tracer particles. The size of the roll and the surface area covered by the kink, respectively, grow and
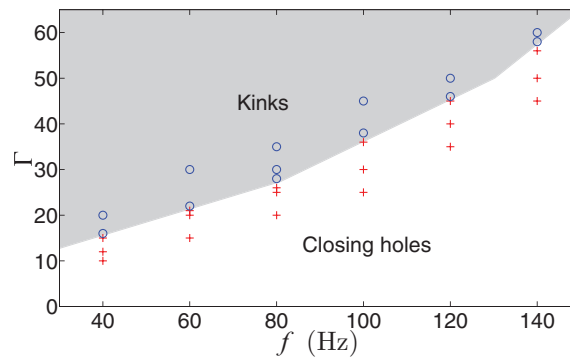
FIG. 11. Phase diagram in the (f, Γ)-plane for a mixture of glitter particles of dimensions $50 \times 50 \times 20$, $50 \times 75 \times 20$, and $50 \times 100 \times 20 \ \mu m^3$. The concentration was $\phi = 0.6$ and the layer depth was fixed to $h = 6$ mm. The grey area is added as a guide to the eye and indicates the region where growing holes grow and kinks are found.

shrink with increasing shaking acceleration. It appears that a higher kink is held in place by a larger convection roll, consistent with the findings of Falcón et al.[18]

Very similar phenomena to the ones described here for the monodisperse polystyrene and the glitter particles have been observed in other suspensions of monodisperse beads[16] and even in vibrated emulsions.[18] In the latter, also stable holes and a delocalized state were found, like in cornstarch suspensions.

V. DISCUSSION AND CONCLUSIONS

In Secs. III and IV, we have mostly focused on the differences between the various particulate suspensions we have studied. We therefore want to start this concluding section by recapitalizing the similarities of which there are quite a few:

- Like every other liquid, suspensions that are vertically vibrated in a container will develop a pattern of surface waves above a certain threshold, the famous Faraday waves.[19] The details of this pattern depend on the frequency and amplitude of the shaking. We have observed these patterns on all suspensions, with the expected period doubling corresponding to half the driving frequency. We also established that the presence of Faraday waves did not significantly interfere with the phenomena discussed in this article.
- Besides the Faraday waves, all presented phenomena require an initial perturbation to be "initiated."
- All presented phenomena overcome hydrostatic pressure: When a hole is created in a Newtonian liquid, gravity will push the liquid back and close the opening. Since in all presented experiments, the holes remain visible for very long times or even grow, the interplay of the suspension properties and the (symmetric) driving works against gravity.
- In all cases particularly dense suspensions are required. Suspensions with lower particle concentrations behave similar to Newtonian liquids and only present closing holes.
- For all patterns that are described in this study, the edges in the suspension (e.g., the rim of the holes) oscillate with the same frequency as that of the driving, with a phase shift. The same is true for a Newtonian liquid, where the rim of the hole, while closing, is also oscillating.
- Many of the suspensions we used appear to be very viscous when at rest, and to flow more easily when shaken. This presumably is a signature of the shear thinning properties that many dense suspensions are reported to have at moderate shear rates.[2–6]

In conclusion, in this paper we have studied extensively the behavior of various vertically vibrating dense suspensions with different particle sizes, shapes, compositions, and distributions. All of these suspensions have in common that there are Faraday waves above a certain threshold and that when a perturbation is created at low shaking strengths and/or low particle concentrations

we observe the formation of a closing hole with oscillating edges, just like what would happen in a viscous Newtonian liquid. However, after an initial perturbation is created in a dense suspension at high shaking strengths we observe a rich variety of phenomena that all overcome hydrostatic pressure. Of all suspensions examined, the cornstarch suspensions present the largest number of different phenomena, which include stable holes, rivers, fingers, and jumping liquid. Moreover, all of these turn out to be unique to cornstarch, since – at least in this study – they have not been observed in the other suspensions.

The other suspensions studied – polydisperse glass beads, polydisperse quartz flour, monodisperse spherical particles, and glitter particles with a narrow size distribution – presented two types of patterns, namely, growing holes, which ultimately develop into kinks, and splitting holes, which split, collide, and merge in a chaotic dynamics. The pattern that is selected is found to be connected to the distribution of particle sizes: Suspensions of particles with a moderate size distribution lead to growing holes, whereas suspensions containing a polydisperse particle distribution (i.e., where large numbers of small particles dominate) lead to splitting holes.

It is particularly intriguing that cornstarch suspensions behave so differently compared to the other suspensions. This either suggests that this behavior is typical for narrowly distributed, edgy particles of the size of cornstarch ($\approx 20\ \mu$m) – for which no alternative made of a different, preferably inorganic, material had been found so far – or that some other undisclosed property of cornstarch is at play.

Our findings raise the important question of why and how different vertically vibrated dense suspensions generate such a variety of different behavior. We believe that this must be due to a coupling of the rheological properties of the particle phase and the liquid. As long as the particles and the liquid move together, i.e., as a single suspension phase of homogeneous composition, no large changes are expected to happen. However, as soon as the liquid is able to move relative to the particle phase, changes in packing fraction will occur. For the (dense) particle phase, it is well established that even a small change in packing fraction may significantly affect the response of the granular phase, even to the point at which it jams completely and does not allow for any flow at all. Such a jammed state may even be reenforced by the presence of the liquid: In the order for the particle phase to unjam, liquid needs to flow back into the jammed region. This flow is limited by the viscous dissipation in the pores, i.e., it is governed by Darcy's law and therefore is expected to depend on the viscosity of the suspending liquid.[8, 12, 20, 21]

The particle size distribution and the shape of the particles enter at this point: The more edgy the particles the easier a small change in packing fraction may locally induce jamming, which in turn is easily relaxed by a modest flow of liquid allowing for small particle rotations and rearrangements that unjam the particle matrix. Such a jamming-unjamming cycle is less easy to create when particles are round and unjamming cannot be effectuated by simple particle rotations. Things become even harder if the particle phase is polydisperse as a result of which the suspension behaves more like a paste in which the smaller phase may flow together with the liquid through the pores.

The details of how the above mechanisms eventually lead to the phenomena discussed in this work is worthy of a thorough quantitative experimental and theoretical investigation. As a first step, we investigated the growth of holes in a sharply peaked particle distribution in a separate article;[22] in general however, such an endeavor lies far beyond the scope of the current article.

ACKNOWLEDGMENTS

APPENDIX: PARTICLE SIZE DISTRIBUTIONS

In this appendix, we will discuss the particle size distributions of the particles used in this study in some greater detail. Here, we use data of the suppliers, whenever available. As a first characteristic, it needs to be noted that particles with a broad size distribution are usually obtained by sieving or sedimentation procedures, and their distributions are usually characterized by the mass fraction a certain size range occupies rather than the number of particles. This in contrast to the more

narrow size distributions where number distributions are more commonly encountered. Evidently, the difference by the two ways of measuring the distribution is small for almost monodisperse or narrow distributions, but increases tremendously when the distributions become very broad.

We have chosen to calculate the average and the spread ($\approx$ two times the standard deviation) using the mass distribution, since the two measures hardly differ for the narrow distributions whereas for the broad distributions a calculation through the number distribution gives far too much emphasis on the smaller fraction leading to unrealistically low values for the average. We will now discuss the distributions starting from the narrowest to the broadest distribution.

1. Monodisperse polystyrene beads (Sec. IV D)

The TS20 dynoseeds (manufacturer MICROBEADS) have the narrowest size distribution of all particles used. We measured from microscopic images that the beads are almost perfectly round with an average particle diameter $\langle d \rangle \approx 22\ \mu$m and a spread of 1 μm (5%). The particles range from 20 to 38 μm where the largest particles are formed by accidental fusion of beads, presumably in the production process. We have also used the TS40 and TS80 dynoseeds which have very similar particle properties, but with average diameters of $\approx$40 and $\approx$80 μm, respectively.

2. Polyester glitter particles (Sec. IV E)

The used glitter particles (manufacturer SIGMUND-LINDNER) consist of rectangles of sizes 50×50, 50×75, and $50 \times 100\ \mu$m^2 cut out of 20 μm thick foil. Each size has a measured spread of around 10%.

3. Cornstarch particles (Sec. IV A)

The size distribution of the cornstarch particles (from several manufacturers) has been measured from microscopic images which yields an average diameter of 17 μm and a spread of 6 μm (30%), where sizes range from 5 to 25 μm.

4. Polydisperse quartz flour (Sec. IV C)

Quartz flour M10 (manufacturer SIBELCO) is one of the broadly distributed particle samples in which the smaller fractions dominate by numbers. The particle sizes range from 0 to 75 μm and the manufacturer provides the following cumulative distribution by mass percentages: $<$4 μm: 10%; $<$30 μm: 50%; $<$75 μm: 90%. This leads to an average diameter of 30 μm and a spread of 45 μm (150%).

5. Polydisperse glass beads (Sec. IV B)

The final batch consists of spherical glass beads (manufacturer SIGMUND-LINDNER) and is the other broadly distributed particle sample. Here, the particle sizes range from 0 to 20 μm and the company gives a distribution by mass percentages: $<$1 μm: 15%; 1–2 μm: 25%; 2–6 μm: 40%; 6–10 μm: 15%; 10–20 μm: 5%. This leads to an average diameter of 4 μm and a spread of 8 μm (200%).

[1] N. Wagner and J. Brady, "Shear thickening in colloidal dispersions," Phys. Today **62**(10), 27 (2009).

[2] H. Barnes, "Shear-thickening (dilatancy) in suspensions of nonaggregating solid particles dispersed in newtonian liquids," J. Rheol. **33**, 329 (1989).

[3] A. Fall, N. Huang, F. Bertrand, G. Ovarlez, and D. Bonn, "Shear thickening of cornstarch suspensions as a reentrant jamming transition," Phys. Rev. Lett. **100**, 018301 (2008).

[4] E. Brown and H. Jaeger, "Dynamic jamming point for shear thickening suspensions," Phys. Rev. Lett. **103**, 086001 (2009).

[5] C. Bonnoit, T. Darnige, E. Clement, and A. Lindner, "Inclined plane rheometry of a dense granular suspension," J. Rheol. **54**, 65 (2010).

[6] E. Brown, N. Forman, C. Orellana, H. Zhang, B. Maynor, D. Betts, J. M. DeSimone, and H. Jaeger, "Generality of shear thickening in suspensions," Nat. Mater. **9**, 220 (2010).

[7] M. van Hecke, "Running on cornflour," Nature (London) **487**, 174 (2012).

[8] S. Waitukaitis and H. Jaeger, "Impact-activated solidification of dense suspensions via dynamic jamming fronts," Nature (London) **487**, 205–209 (2012).

[9] A. Fall, F. Bertrand, G. Ovarlez, and D. Bonn, "Shear thickening of cornstarch suspensions," J. Rheol. **56**, 575–591 (2012).

[10] C. Bonnoit, J. Lanuza, A. Lindner, and E. Clement, "Mesoscopic length scale controls the rheology of dense suspensions," Phys. Rev. Lett. **105**, 108302 (2010).

[11] E. B. White, M. Chellamuthu, and J. Rothstein, "Extensional rheology of a shear-thickening cornstarch and water suspension," Rheol. Acta **49**, 119–129 (2010).

[12] S. von Kann, J. Snoeijer, D. Lohse, and D. van der Meer, "Nonmonotonic settling of a sphere in a cornstarch suspension," Phys. Rev. E **84**, 060401(R) (2011).

[13] B. Liu, M. Shelley, and J. Zhang, "Focused force transmission through an aqueous suspension of granules," Phys. Rev. Lett. **105**, 188301 (2010).

[14] F. Merkt, R. Deegan, D. Goldman, E. Rericha, and H. Swinney, "Persistent holes in a fluid," Phys. Rev. Lett. **92**, 184501 (2004).

[15] R. Deegan, "Stress hysteresis as the cause of persistent holes in particulate suspensions," Phys. Rev. E **81**, 036319 (2010).

[16] H. Ebata, S. Tatsumi, and M. Sano, "Expanding holes driven by convectionlike flow in vibrated dense suspensions," Phys. Rev. E **79**, 066308 (2009).

[17] H. Ebata and M. Sano, "Self-replicating holes in a vertically vibrated dense suspension," Phys. Rev. Lett. **107**, 088301 (2011).

[18] C. Falcón, J. Bruggemann, M. Pasquali, and R. Deegan, "Localized structures in vibrated emulsions," Europhys. Lett. **98**, 24002 (2012).

[19] M. Faraday, "On a peculiar class of acoustical figures; and on certain forms assumed by groups of particles upon vibrating elastic surfaces," Philos. Trans. R. Soc. London **121**, 299–340 (1831).

[20] E. Brown, N. Rodenberg, J. Amend, A. Mozeikac, E. Steltzc, M. R. Zakin, H. Lipson, and H. Jaeger, "Universal robotic gripper based on the jamming of granular material," Proc. Natl. Acad. Sci. U.S.A. **107**, 18809–18814 (2010).

[21] S. von Kann, J. Snoeijer, and D. van der Meer, "Velocity oscillations and stop-go cycles: The trajectory of an object settling in a cornstarch suspension," Phys. Rev. E **87**, 042301 (2013).

[22] S. von Kann, M. van de Raa, and D. van der Meer, "Hole dynamics in vertically vibrated suspensions," e-print arXiv:1312.4040.